Rabbit Skeletal Myosin Heads in Solution, As Observed by Ultracentrifugation and Freeze–Fracture Electron Microscopy: Dimerization and Maximum Chord

Nacima Bachouchi, Annette Gulik,‡ Manuel Garrigos, and Jean E. Morel*

Département de Biologie, Service de Biophysique, CEN-Saclay, 91191 Gif-sur-Yvette Cédex, France, and Ecole Centrale des Arts et Manufactures, Département de Chimie, Grande Voie des Vignes, 92290 Châtenay-Malabry, France

Received January 18, 1985

ABSTRACT: The use of analytical ultracentrifugation and freeze–fracture electron microscopy in solution allowed us to observe the monomeric and dimeric forms of Mg·S1. This subfragment of the myosin molecule contains the LC2 light chain and is comparable to a "native" myosin head. Sedimentation–diffusion equilibrium ultracentrifugation shows that it is necessary to use slightly different conditions in order to obtain a pure Mg·S1 dimer, as compared to the case of chymotryptic S1 (LC2-free S1). For example, in a buffer leading to a complete dimerization of chymotryptic S1, Mg·S1 is only in the form of a monomer–dimer mixture, with comparable proportions of monomer and dimer. The freeze–fracture technique, applied to solutions containing Mg·S1 or chymotryptic S1, revealed that the monomeric species both have the same maximum chord (about 120 Å) and that both dimeric species also have the same maximum chord (about 250 Å). The maximum chord of the monomer is comparable to the surface-to-surface spacing between the myosin and actin filaments, in a fiber at the slack length. In sharp contrast this chord is higher than this spacing in a stretched fiber. The consequences of this fact are discussed, with particular reference to the sarcomere length–tension relationship.

It has been shown recently that chymotryptic subfragment 1 (S1)[1] from rabbit skeletal muscle myosin, i.e., LC2-free S1, exists in the form of a monomer–dimer mixture, whose equilibrium constant is a function of the hydrostatic pressure, the temperature, and the composition of the buffer (Morel & Garrigos, 1982a). At atmospheric pressure, in a benign buffer, S1 is mostly in the form of a monomer, but at low ionic strength, at high pH, and in the presence of a Mg–(phosphate compound), S1 exists in the form of an almost pure dimer. Here, we examine the characteristics of Mg·S1 (which contains LC2), particularly to determine whether it can also undergo a dimerization. This problem is important since Mg·S1 closely ressembles a "native" myosin head, and in view of the recent model proposed for the structure of the thick filaments in vivo (Morel & Garrigos, 1982b), it is necessary to see whether intact myosin heads can interact in vitro. Moreover, dimerization of the myosin heads might be relevant to the mechanism of contraction itself (Morel & Gingold, 1979). We have not studied all the parameters that affect the monomer–dimer equilibrium constant. We have focused on the conditions in which Mg·S1 is in the form of a pure monomer or a pure dimer and have established the maximum chord of Mg·S1 in each case. This is also a major problem, since it is necessary to know the exact distance between the extremity of a myosin head and the surface of the neighboring actin filament, in order to have a more rigorous approach of the molecular mechanisms of muscle contraction. For LC2-free S1, it has been found, at 1–5 °C and in solution that the maximum chord of the monomer is about 120 Å (Mendelson, 1982; Mendelson & Kretzschmar, 1980; Garrigos et al., 1983). Using X-ray scattering, Mendelson (1982) has found that Mg·S1, under the same conditions, has the same maximum chord (120 Å). In order to try to measure this chord for both samples (LC2-free S1 and Mg·S1), we used the technique of freeze–fracture electron microscopy of protein solutions (Le Maire et al., 1981; Gulik et al., 1982). As pointed out by Garrigos et al. (1983), conventional electron microscopy leads to dehydration of the heads, which apparently results in considerable distortions of the structures. In this context, we consider that the value of 190 Å for the length of a myosin head (Elliott & Offer, 1978) is too large as compared with the 120 Å found in solution [for a complete discussion on this problem, see Garrigos et al. (1983)]. The technique used here leads to results in good agreement with those obtained by other methods upon solutions of LC2-free S1 and Mg·S1 (Mendelson, 1982; Mendelson & Kretzschmar, 1980; Garrigos et al., 1983). Using the same technique, we have estimated the maximum chord of the dimer.

Materials and Methods

Preparation of Chymotryptic S1 and Mg·S1. Mg·S1 from rabbit skeletal muscle myosin was prepared according to the standard procedure described by Margossian & Lowey (1982). Before use for freeze–fracture, Mg·S1 was purified and concentrated up to 10–15 mg/mL by ammonium sulfate fractionation and precipitation, as described by Margossian & Lowey (1973). The light precipitate obtained at 42% saturated ammonium sulfate (4 °C) was discarded by centrifugation at 30000 rpm for 15 min (in a Beckman 50Ti rotor). The supernatant was brought to 58% saturated ammonium sulfate and centrifuged at 30000 rpm for 15 min (50Ti). The pellet was separated into two equivalent volumes and redissolved in

* Address correspondence to this author at the Département de Biologie, Service de Biophysique, CEN-Saclay, 91191 Gif-sur-Yvette Cédex, France.

‡ CNRS, Centre de Génétique Moléculaire, 91190 Gif-sur-Yvette, France.

[1] Abbreviations: ADP, adenosine 5′-diphosphate; AMP-PNP, adenyl-5′-yl imidodiphosphate; $NaDodSO_4$, sodium dodecyl sulfate; DTT, dithiothreitol; BTP, Bis-tris-propane [1,3-bis[[tris(hydroxymethyl)-methyl]amino]propane]; EGTA, ethylene glycol bis(β-aminoethyl ether)-*N,N,N′,N′*-tetraacetic acid; chymotryptic S1 or S1, LC2-free myosin subfragment 1; Mg·S1, myosin subfragment 1 containing LC2.

0006-2960/85/0424-6305$01.50/0

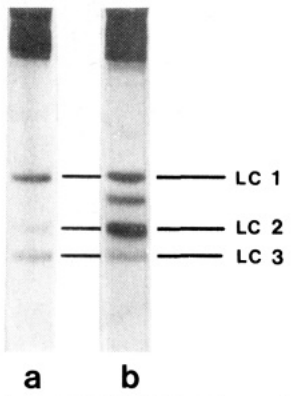

FIGURE 1: Discontinuous $NaDodSO_4$–polyacrylamide gel electrophoreses of chymotryptic S1 (a) and Mg·S1 (b), prepared according to the standard procedures of Margossian & Lowey (1982). Note the cleavage at the level of LC1 in Mg·S1, which is a well-known result (Margossian et al., 1981). The cleavages at the level of the heavy chains (Margossian et al., 1981) are not seen, owing to the high protein concentrations used, in order to clearly see the light chains. In spite of these cleavages, the S1 species are homogeneous under nondenaturating conditions (Margossian et al., 1981).

either buffer A (115 mM KCl, 50 mM imidazole, 2 mM DTT, and 2 mM $MgCl_2$, pH 6.9) or buffer B (0 mM KCl, 50 mM imidazole, 2 mM DTT, 2 mM DTT, and 8 mM $MgCl_2$, pH 7.5). $MgCl_2$ was present in both buffers, in order to obviate eventual dissociation of LC2 from Mg·S1. The two concentrated Mg·S1 solutions were extensively dialyzed against buffer A or B. After dialysis, 5 mM AMP-PNP was added to the Mg·S1 solution in buffer B (buffer B′ = buffer B + 5 mM AMP-PNP). Before use, the two solutions were clarified by centrifugation at 40000 rpm for 30 min (50Ti). This procedure led to extremely clear solutions and eliminated possible aggregates due to some kind of salting out in buffer B′ (presence of 8 mM $MgCl_2$). We also concentrated the Mg·S1 solutions by filtration on an Amicon XM-50 filter. After the same clarification procedure, the results obtained were the same. Finally, we also obtained the same results by concentrating the Mg·S1 solutions by ultracentrifugation in a Beckman SW 60 rotor (duration 10 h at 50000 rpm; the concentrated solution was present at the bottom of the tubes). Owing to the rapidity of the ammonium sulfate concentration method, we routinely used this procedure.

For sedimentation–diffusion equilibrium ultracentrifugation, no concentration step was necessary, since the Mg·S1 concentrations were only 0.1, 0.38, and 1.0 mg/mL (see below). However, we did some purification experiments by ammonium sulfate, by eliminating the light precipitate obtained at 42% saturation. The results obtained with this procedure were exactly the same as those obtained without purification, indicating that the amount of contaminants (e.g., myokinase) is extremely low.

In order to calibrate the freeze–fracture technique, we also made use of chymotryptic S1, whose properties and dimension are now well-known (Mendelson, 1982; Mendelson & Kretzschmar, 1980; Garrigos et al., 1983). This species was prepared according to the standard procedure described by Margossian & Lowey (1982). It was concentrated only by the ammonium sulfate method, described above for Mg·S1. The final buffers were repectively buffer C (150 mM KCl, 50 mM KCl, 50 mM imidazole, and 2 mM DTT, pH 6.9) and buffer B′ (see above). In all cases, the S1 and Mg·S1 solutions were kept on ice before use and used immediately after preparation.

Characterization of Chymotryptic S1 and Mg·S1. As shown on Figure 1, the discontinuous $NaDodSO_4$–polyacrylamide gel electrophoreses were characteristic of chymotryptic S1 (absence of LC2) and Mg·S1 (presence of LC2).

We tested the MgATPase activities of both species, at 20 °C. In fact, although these activities are very low, they are the most important, since they are enhanced by F-actin. These functional tests were carried out by using the fluorometric technique described by Mandelkow & Mandelkow (1973). In all buffers, we replaced imidazole by BTP, in order to obviate a possible light absorption by imidazole. For both S1 species, the activities were the same, within the limits of the experimental error, which is not unexpected, since LC2 plays a minor role in the MgATPase activity (Trentham et al., 1972; Weeds & Taylor, 1975). Under the following conditions, 0 mM KCl, 2 mM $MgCl_2$, 2 mM DTT, 50 mM BTP, pH 7.4, 0.1 mM EGTA (in order to complex traces of calcium), 2 μM S1, and 30 μM ATP, we found an activity of about 0.050 s^{-1}, which is in good agreement with the activities reported by Trentham et al. (1972) (0.040–0.060 s^{-1}, at 21–25 °C, pH 8.0, per catalytic center in heavy meromyosin) and Weeds & Taylor (1975) (0.040–0.050 s^{-1} for both LC2-free S1 and Mg·S1, at pH 8.0). Interestingly, however, we observed that in buffer A or C, plus 30 μM ATP and 0.1 mM EGTA, where the species are in the monomeric form (see below), the MgATPase activity was only 0.014 ± 0.001 s^{-1} (mean of 16 experiments). In buffer B, plus 30 μM ATP and 0.1 mM EGTA, where the species are in the dimeric form (see below), the MgATPase was 0.047 ± 0.001 s^{-1} (mean of six experiments). These results are not artifactual, since by replacing buffer B by buffer A or C, on a given protein solution, the MgATPase activity systematically drops from 0.047 to 0.014 s^{-1}. These tests indicate that the monomer and the dimer behave differently. This behavior is a further confirmation that the dimer exists (Morel & Garrigos, 1982a,b; see below). Moreover, we conclude that our S1 species are functionally intact and well-defined. A full paper on the MgATPase activity of S1 will be published later.

Sedimentation–Diffusion Equilibrium Ultracentrifugation. The experiments were carried out as previously described (Morel & Garrigos, 1982a,b), in an Yphantis six-channel cell and using the Rayleigh interference optical system. In order to minimize the effects of hydrostatic pressure, we used an extremely short column length (1 mm). The other conditions were the following: temperature 4 °C, rotor speed 10000 rpm, protein loading concentration 0.38 mg/mL, (unless specified), duration of the experiments 24 h.

Freeze–Fracture in Solution. It has been shown recently that freeze–fracture electron microscopy can be used successfully to study the morphology of proteins and other biological molecules in solution (Le Maire et al., 1981; Gulik et al., 1982). The protein solutions, containing 30% glycerol, were conventionally frozen–fractured and replicated with tungsten–tantalum [for more details, see Gulik et al. (1982)]. The molecules, observed under the electron microscope, represent portions of the molecules exposed above the surface of ice by the fracture. The distribution of the particle sizes reflects the varying degrees of exposure and orientation of the protein, and it can be correlated with the shape and dimensions of the proteins (Le Maire et al., 1981; Gulik et al., 1982). One of the major drawbacks of this technique in visualizing molecules is that they are embedded, in random spatial configuration, in ice. However, as we shall see below, the technique is powerful in determining, at least, the maximum chord of a molecule.

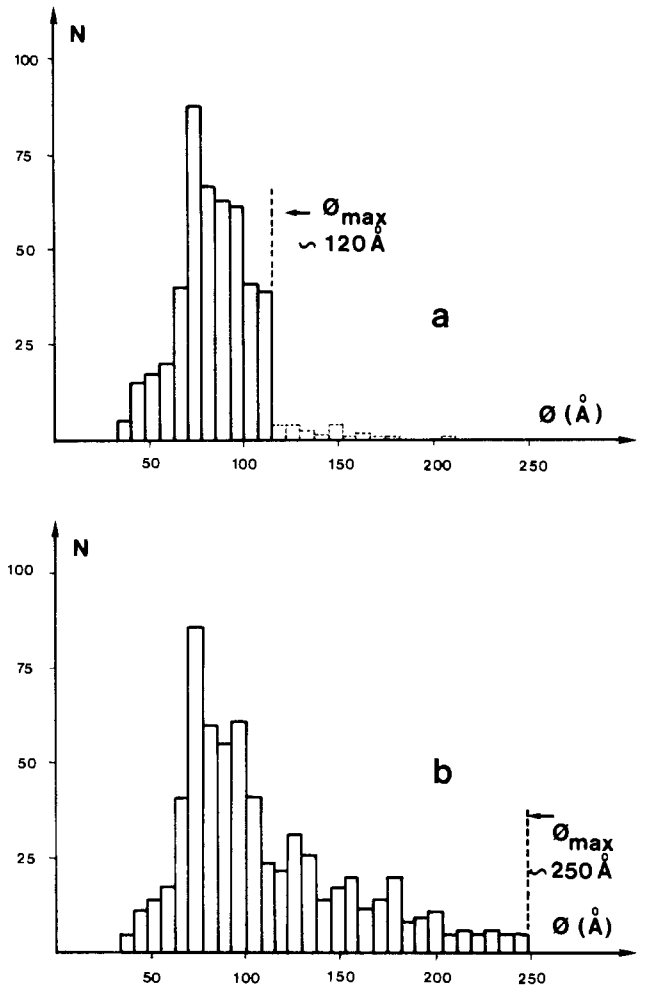

FIGURE 2: Histograms representing the size distributions of the LC2-free S1 monomer and dimer. The electron micrographs corresponding to LC2-free S1 are quite similar to those presented on Figure 3. The principle of particle size measurements is described under Materials and Methods. (a) Histogram corresponding to the LC2-free S1 monomer. The dashed part of the histogram corresponds to some contamination by dimeric particles (see also legend to Figure 3). The choice of the cutoff at 120 Å is supported by the sudden large decrease in the number of particles counted around this value. (b) Histogram corresponding to the LC2-free S1 dimer. Note the large asymmetry of this histogram and the maximum chord of about 250 Å. Here again, the cutoff is well-defined, since above 250 Å no molecule can be counted. The "trailing end" of the histogram corresponding to large values of ϕ clearly indicates that few dimers are visualized lying lengthwise, which is expected for asymmetrical molecules [see Gulik et al. (1982)].

Since the freeze–fracture technique used here is rather new, it is important to establish that the results obtained in our case accurately reflect the morphology of Mg·S1. For this purpose, it is necessary to compare the results with those obtained by using other methods. This has been done for a large number of known molecules (Le Maire et al., 1981; Gulik et al., 1982), but not for S1.

Since LC2-free S1 in solution is a well-known molecule (see above), we applied the freeze–fracture technique to the monomer (buffer C) and the dimer (buffer B′). The results of the electron microscopic observations were quite similar to those presented in Figure 3. From the micrographs, we could draw the two histograms presented in Figure 2 using the following procedure. N is the number of particles counted. ϕ is the dimension of the particles, as measured in a direction perpendicular to their shadow. The measurements of ϕ were done by using a finely graduated ruler placed on a large field magnifier (2×). The precision of individual measurements was estimated to be ±0.1 mm, which corresponds to an error in particle size of ±7.4 Å. The different classes of values of ϕ were chosen as 7.4 Å wide. The measured maximum chord of the monomer, determined from the first histogram (Figure 2a), is about 120 Å, in agreement with previous determinations (Mendelson, 1982; Mendelson & Kretzschmar, 1980; Garrigos et al., 1983). Further, we deduce that, for S1, the thickness of the metal cap is within the limits of the experimental error. In fact, the monomer maximum chord as measured on our pictures was 126 ± 7.4 Å (the 7.4 Å corresponding to the error of ±0.1 mm in the measurement of particle size; as discussed). As we know that the W–Ta deposit is small (much smaller than the Pt–C commonly used) and taking into account the precision of the particle size measurements, we adopted a value of 120 Å for the monomer maximum chord. Therefore, no correction was made for the metal cap thickness. Concerning the dimer, the second histogram shows that the maximum chord is about 250 Å (Figure 2b), i.e., about twice the maximum chord of the monomer. The sedimentation coefficient of the dimer (6.05 S) is not drastically different from that of the monomer (5.05 S) (Morel & Garrigos, 1982a). This small difference can be explained only by the presence of an end-to-end dimer (Morel & Garrigos, 1982a). The maximum chord of 250 Å found by the freeze–fracture technique is in agreement with this previous conclusion.

In conclusion, the freeze–fracture technique, previously shown to be useful for a variety of molecules in solution (Le Maire et al., 1981; Gulik et al., 1982), is also suitable for the study of S1, both in the monomeric and in the dimeric forms.

Results

Sedimentation–Diffusion Equilibrium Ultracentrifugation on Mg·S1. Mg·S1 was in the form of a pure monomer in buffer A (M_r 127 000) and in the form of a pure dimer in buffer B′ (M_r 250 000). These values were obtained by taking $\bar{V}$ = 0.740 mL/g for the monomer and 0.725 mL/g for the dimer (Morel & Garrigos, 1982a). Note that the molecular weight of the LC2-free S1 is 107 000 (Morel & Garrigos, 1982a; Garrigos et al., 1983) and that the difference between 127 000 and 107 000 is related to the presence of LC2 in Mg·S1 (M_r 18 000–19 000), as clearly shown in Figure 1. No difference in the molecular weights was observed when 30% glycerol was added to the buffers (glycerol is necessary for freeze–fracture; see Materials and Methods). The calculations of the molecular weights in the presence of 30% glycerol were done by using the above values of $\bar{V}$ and by adding 0.080 g/mL to the densities of the buffers. Note that buffer B′ is slightly different from the buffer that led to a pure dimer in the case of LC2-free S1 [20 mM KCl, 5 mM $MgCl_2$, 50 mM imidazole, 2 mM ADP, and 2 mM DTT, pH 7.5; see Morel & Garrigos (1982a)]. In fact, when this buffer was used, we found only a monomer–dimer mixture of Mg·S1, with an equilibrium constant K = 1.2 mL/mg, which corresponds to about 25% dimer and 75% monomer at c = 0.38 mg/mL. If the loading concentration of 0.38 mg/mL is replaced by 0.1 or 1.0 mg/mL, we found the same values of K in this buffer, within the limits of the experimental errors (K = 1.2 ± 0.1 mL/mg). This is a criterion of reversibility (Morel & Garrigos, 1982a); i.e., the Mg·S1 monomer–dimer equilibrium is reversible, as is the case for LC2-free S1. We see from the above results that it is necessary to use slightly different conditions in order to induce a complete dimerization of Mg·S1, as compared with LC2-free S1. Here the KCl content was lowered to zero (instead of 20 mM), the $MgCl_2$ content was increased up to 8 mM (instead of 5 mM), and ADP was replaced by AMP-PNP, with an increased concentration (5

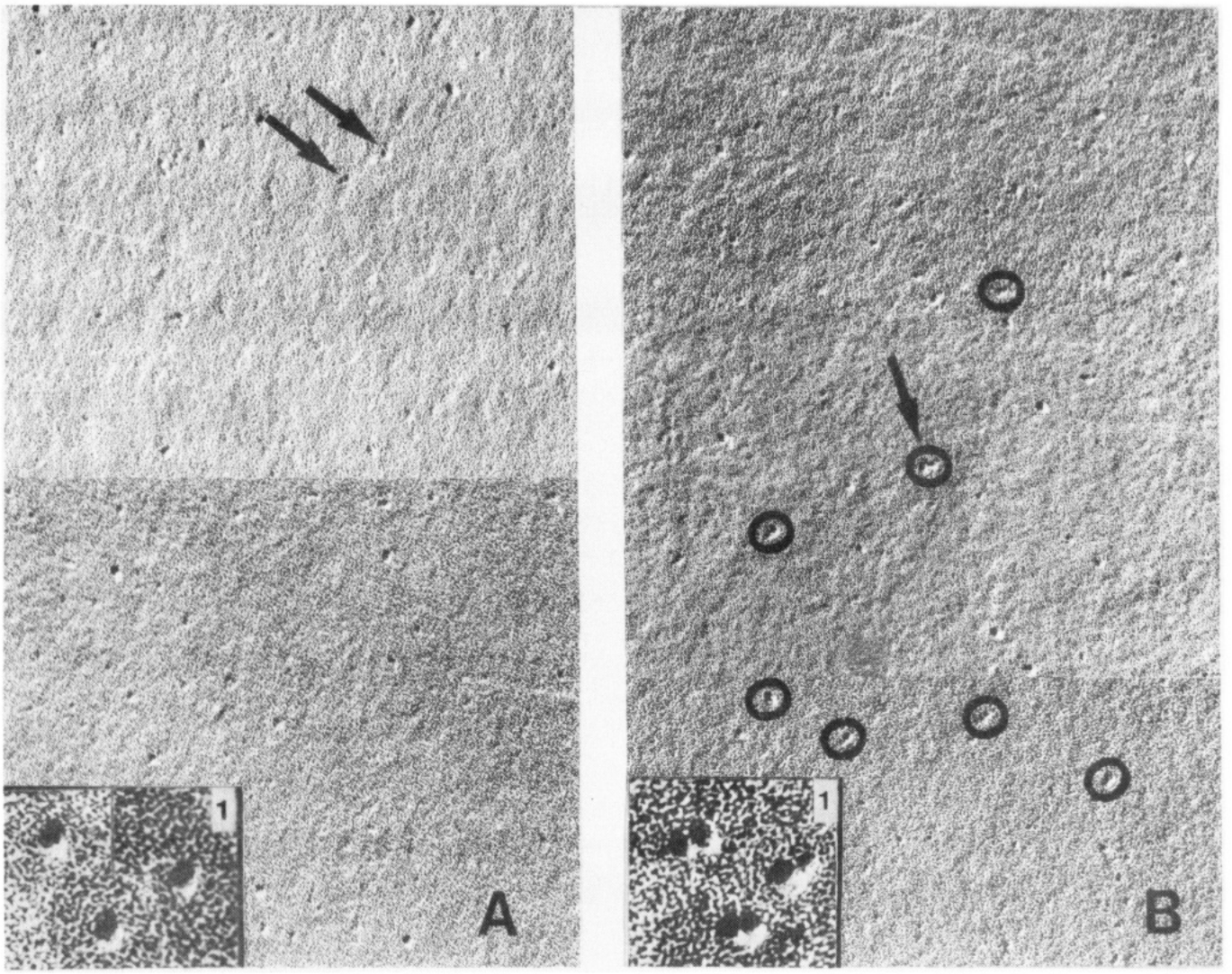

FIGURE 3: Freeze–fracture images of Mg·S1. (A) Mg·S1 in the monomeric form (buffer A; see Materials and Methods). The arrows indicate some dimeric particles. This contamination is due to the high concentration needed for the freeze–fracture electron microscopy observations (7–10 mg/mL after addition of 30% glycerol), as compared to those needed for ultracentrifugation (less than 1 mg/mL). (B) Mg·S1 in the dimeric form (buffer B′; see Materials and Methods). The circles indicate some dimers lying approximately along their long axis. The arrow indicates a dimer in which the axes of the two protomers make an angle different from 180° (110–120°). We do not know whether this observation is genuine or not. Magnification 135000×. Insets A.1 and B.1: some monomeric and dimeric particles with a magnification of 400000×. As expected, the mean number of particles observed on the photographs of the monomer was about twice that observed in the case of the dimer. For example, for a series of seven micrographs, 103 particles per micrograph were counted in the case of the monomer and only 54 in the case of the dimer (m/d = 1.91). This simple result is a good verification of the existence of the dimer.

mM AMP-PNP instead of 2 mM ADP). Therefore, Mg·S1 dimerizes to a lesser extent than chymotryptic S1. However, the present and previous experimental studies show that LC2 is not involved qualitatively in the dimerization process but that this light chain seems to modulate the monomer–dimer equilibrium constant.

Freeze–Fracture on Mg·S1. Figure 3 shows freeze–fracture images of Mg·S1 in the monomeric state (buffer A; Figure 3A) and in the dimeric state (buffer B′; Figure 3B). The corresponding histograms of the particle sizes are shown in Figure 4. The maximum dimension for the monomer can be estimated to be about 120 Å, in agreement with previous determinations made in solution for the maximum chord of both LC2-free S1 and Mg·S1 (Mendelson, 1982; Mendelson & Kretzschmar, 1980; Garrigos et al., 1983). The maximum chord of the dimer can be estimated to be about 250 Å, i.e., twice the maximum chord for the monomer. Moreover, the histogram for the dimer is characteristic of an elongated molecule (Figure 2; Gulik et al., 1982). Both the maximum chord and the shape of the histogram strongly suggest that the Mg·S1 dimer is predominantly end-to-end, as is the case for LC2-free S1.

Discussion

Case of the Monomer and the Myosin Heads. Some parameters of S1 have been determined by hydrodynamic methods; they take into account the hydration of the entire molecule, which is very high in the case of S1 (Garrigos et al., 1983). The major axis of the equivalent prolate ellipsoid has been estimated to be between 140 and 170 Å (mean value 155 Å) by Kinosita et al. (1984) or 156 Å by Garrigos et al. (1983). From small-angle X-ray scattering in solution, Mendelson (1982) has found that the maximum chord of both LC2-free S1 and Mg·S1 is 120 ± 10 Å. By comparing the hydrodynamic and the X-ray scattering data, Garrigos et al. (1983) have shown that the 156 Å of the hydrated LC2-free S1 monomer corresponds to a maximum chord of 119 Å. These results are in good agreement with the value obtained in the present study. Furthermore, our result is compatible with that of 148 ± 15 Å obtained by Labbé et al. (1984) from rotary shadowing of molecules dried from glycerol, a technique

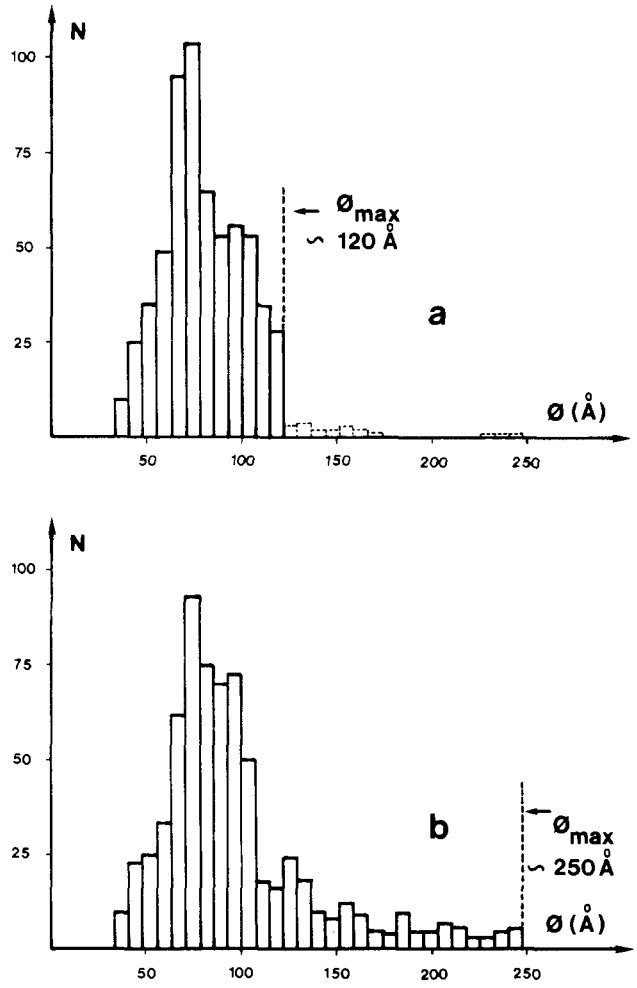

FIGURE 4: Histograms representing the size distributions of particles in the case of Mg·S1. N is the number of particles counted. ϕ is the dimension of the particles as measured in a direction perpendicular to their shadow. The measurements of ϕ were done as described under Materials and Methods. (a) Mg·S1 in the monomeric form. The dashed part of the histogram corresponds to some contamination by dimeric particles (see also Figure 2). (b) Mg·S1 in the dimeric form. Note that when the dimer was clearly observed as built up of two distinct protomers (Figure 3B), ϕ corresponded to the distance between the extremities of the dimer. In both figures, ϕ_{max} represents the maximum chord and the cutoff in both cases of the monomer, and the dimer is clearly observed (see also Figure 2). The exact meaning of the maximum in N is not known. The diameter of the equivalent unhydrated sphere is given by $2R = 2[3M_r\bar{V}/(4\pi N_A)]^{1/3}$. $2R$ can be calculated for the monomer (M_r 127 000; $\bar{V}$ = 0.740 mL/g). The axial ratio p of the equivalent prolate ellipsoid is given by $p = (\phi_{max}/2R)^{3/2}$, which leads, for the monomer, to a p of about 2.4, in agreement with previous determinations [2.3 (Garrigos et al., 1983; Labbé et al., 1984) (in this last case the 20-Å correction was applied to the major and minor axes); 2.2–2.9 (Kinosita et al., 1984)].

known to produce images that overestimate the dimensions of molecules (Tyler & Branton, 1980).

The recent procedure of freeze-drying molecules on mica flakes has been used for the whole myosin molecule (Heuser, 1983). It is difficult to measure the dimension of the heads with the few molecules shown on Figure 14a of this study. The maximum dimension of the heads can be estimated at around 170 Å (after 20-Å correction for Pt thickness; 12 heads measured), a value larger than ours. This might be explained by some flattening and deformation during the drying of the heads, which have a particularly high degree of hydration (Garrigos et al., 1983). The same remark also holds for the value of 160 Å found by Winkelman et al. (1985) for avian skeletal Mg·S1, in the crystallized form. This problem has been already discussed in detail by Garrigos et al. (1983).

It appears that the geometry of LC2-free S1 and Mg·S1 is the same. This observation, valid for the rabbit, is not in agreement with that of Vibert & Craig (1982) and Flicker et al. (1983) on scallop S1. EDTA·S1 (absence of the Ca^{2+} regulatory chain) would have a maximum chord of 105 ± 15 Å and Ca·Mg·S1 (presence of the Ca^{2+} regulatory chain) would have a maximum chord of 180 ± 25 Å, i.e., a considerable difference of 75 ± 40 Å. This large discrepancy between rabbit and scallop has been already discussed by Mendelson (1982). To this discussion we must add the fact that conventional electron microscopy can lead to considerable distortions [see Garrigos et al. (1983)]. Therefore, we have more confidence in the results obtained directly in solution by means of X-ray scattering or by means of our technique of freeze–fracture, both approaches giving the same results. However, we do not dismiss the fact that scallop S1 and rabbit S1 might behave differently.

Finally, the similarity in the geometry of LC2-free S1 and Mg·S1 would indicate that LC2 is localized in the hole present in the myosin head and located at one extremity of this head (Garrigos et al., 1983).

Case of the Dimer. The shape of the histograms and the comparison of the maximum chord of the monomer and the dimer strongly suggest an end-to-end association of the protomers in the dimer. However, this conclusion does not rule out the possibility of the presence of some amount of side-by-side dimers or intermediary arrangements. This is also the case with LC2-free S1, but the small difference between the sedimentation coefficient of the dimer (6.05 S) and that of the monomer (5.05 S) indicates that the end-to-end dimer is largely predominant (Morel & Garrigos, 1982a). In the case of Mg·S1, one may argue that we have not determined the sedimentation coefficients. The nature of the dimer might be different in the case of Mg·S1 and LC2-free S1. We do not favor this possibility, since Margossian et al. (1975) have shown that, under standard conditions, the two species have the same sedimentation coefficients (5.80 S, which corresponds to a large proportion of dimer). We conclude that the Mg·S1 dimer is predominantly end-to-end, as is the LC2-free S1 dimer. Although the procedures used by Winkelman et al. (1985) seem to introduce distortions in the shape and size of Mg·S1 (see above), these authors have also found, on crystallized Mg·S1, the presence of an end-to-end dimer.

Conclusion

This study is of particular interest in that it allows good visualization of both LC2-free S1 and Mg·S1. The dimer is clearly seen, and we obtain good estimates of the maximum chords of both the monomers and the dimers. The Mg·S1 dimer is end-to-end, as is the case for LC2-free S1. Moreover, concerning the monomer, we confirm that the presence or absence of LC2 has no detectable influence on the geometry of the head, at least in the case of rabbit skeletal muscle. Further, (i) there is a good agreement among the results obtained by freeze–fracture and other studies in solution, contrary to some results obtained with other microscopic techniques (e.g., negative staining or Pt-shadow casting), and (ii) the two protomers in the dimer are not significantly different from the individual monomers, since the maximum chord of the end-to-end dimer is twice that of the monomer.

Finally, from the experiments of Elliott et al. (1963), we deduce that the center-to-center distance between a myosin and an actin filament, in the case of the rabbit skeletal muscle, is about 255 Å at the slack length (sarcomere length about 2.2 μm). The radius of the myosin filament backbone is 80 Å (Morel & Garrigos, 1982b) and that of the actin filament

50 Å (Egelman & Padrôn, 1984). Thus, the surface-to-surface spacing between a thick and a thin filament is about 125 Å, which is extremely close to the maximum chord of a myosin head (120 Å). The exact angle between a myosin head and the thick filament axis, in relaxation, is not well-known. However, if it is assumed to be 90°, as is usual, we see that the extremity of the myosin head, in vivo and at the slack length, is extremely close to the surface of the neighboring actin filament. At a sarcomere length of 3.3 μm, the surface-to-surface spacing becomes only about 90 Å, which is significantly lower than 120 Å. We conclude that, by stretching the muscle fiber, the myosin heads are compressed and/or tilted with respect to the position they have at the slack length. For a stretched, contracting fiber, the number of cross bridges is lower than at full ovelap between the myofilaments, but the conformation of the cross bridges is also necessarily mechanically altered by stretching. For these reasons, we consider that the problem of the sarcomere length–tension relationship, for example, is more complicated than expected, as recently shown (Morel, 1984a). On the other hand, dimerization of the myosin heads seems to be relevant with the energetics of a whole contracting muscle (Morel, 1984b) and, maybe, with the mechanism of contraction itself (Morel & Gingold, 1979).

ACKNOWLEDGMENTS

We are indebted to Dr. G. Batelier for having performed the ultracentrifugation experiments and to Dr. F. Guillain for valuable advice. We are grateful to Drs. L. P. Aggerbeck and T. Gulik-Krzywicki for helpful discussions. Thanks are due to Dr. J. C. Dedieu and Mrs. O. Batail for their help in the tedious work of particle size measurements.

REFERENCES

Egelman, E. H., & Padrôn, R. (1984) *Nature (London) 307*, 56–58.
Elliott, A., & Offer, G. (1978) *J. Mol. Biol. 123*, 505–519.
Elliott, G. F., Lowy, J., & Worthington, R. C. (1963) *J. Mol. Biol. 6*, 295–305.
Flicker, P. F., Walliman, T., & Vibert, P. (1983) *J. Mol. Biol. 169*, 723–741.
Garrigos, M., Morel, J. E., & Garcia de la Torre, J. (1983) *Biochemistry 22*, 4961–4969.
Gulik, A., Aggerbeck, L. P., Dedieu, J. C., & Gulik-Krzywicki, T. (1982) *J. Microsc. 125*, 207–213.
Heuser, J. E. (1983) *J. Mol. Biol. 169*, 155–195.
Kinosita, K., Jr., Ishiwata, S., Yoshimura, H., Asai, H., & Ikegami, A. (1984) *Biochemistry 23*, 5963–5975.
Labbé, J. P., Bertrand, R., Audemard, E., Kassab, R., Walzthöny, D., & Walliman, T. (1984) *Eur. J. Biochem. 143*, 315–322.
Le Maire, M., Møller, J. V., & Gulik-Krzywicki, T. (1981) *Biochim. Biophys. Acta 643*, 115–125.
Mandelkow, E. M., & Mandelkow, E. (1973) *FEBS Lett. 33*, 161–163.
Margossian, S. S., & Lowey, S. (1973) *J. Mol. Biol. 74*, 313–330.
Margossian, S. S., & Lowey, S. (1982) *Methods Enzymol. 85*, 55–71.
Margossian, S. S., Lowey, S., & Barshop, B. (1975) *Nature (London) 258*, 163–169.
Margossian, S. S., Stafford, W. F., III, & Lowey, S. (1981) *Biochemistry 20*, 2151–2155.
Mendelson, R. A. (1982) *Nature (London) 298*, 665–667.
Mendelson, R. A., & Kretzschmar, K. M. (1980) *Biochemistry 19*, 4103–4108.
Morel, J. E. (1984a) *Prog. Biophys. Mol. Biol. 44*, 47–71.
Morel, J. E. (1984b) *Prog. Biophys. Mol. Biol. 44*, 73–96.
Morel, J. E., & Gingold, M. (1979) *Acta Protozool. 18*, 179 (Abstract).
Morel, J. E., & Garrigos, M. (1982a) *Biochemistry 21*, 2979–2986.
Morel, J. E., & Garrigos, M. (1982b) *FEBS Lett. 149*, 8–16.
Trentham, D. R., Bardley, R. G., Eccleston, J. F., & Weeds, A. G. (1972) *Biochem. J. 126*, 635–644.
Tyler, J. M., & Branton, D. (1980) *J. Ultrastruct. Res. 71*, 95–102.
Vibert, P., & Craig, R. (1982) *J. Mol. Biol. 157*, 299–319.
Weeds, A. G., & Taylor, R. S. (1975) *Nature (London) 257*, 54–56.
Winkelman, D. A., Mekeel, H., & Rayment, I. (1985) *J. Mol. Biol. 181*, 487–501.